Time-dependent close-coupling calculations for the electron-impact ionization of helium

M. S. Pindzola and F. J. Robicheaux
Department of Physics, Auburn University, Auburn, Alabama 36849
(Received 22 October 1999; published 7 April 2000)

Electron-impact ionization cross sections for helium are calculated using time-dependent close-coupling theory. In a frozen-core approximation, the wave function for the three-electron system is expanded in terms of two-electron wave functions which fully describe the ejected and scattered electrons at all times following the collision. The resulting close-coupled partial differential equations for the two-electron radial wave functions include a direct and a local approximation to the exchange interactions with the remaining core electron. By direct projection of the time-dependent wave functions onto continuum lattice eigenstates, both ejected energy differential and total integrated cross sections are extracted. The agreement between theory and previous experimental measurements for helium is excellent.

PACS number(s): 34.80.Dp

I. INTRODUCTION

For many atoms and their ions the total electron-impact ionization cross section is dominated by the direct ''knock-out'' ionization process. The final state of such a direct process finds two electrons moving in the long-range Coulomb field of a third body. Only in the last few years have nonperturbative theoretical collision methods been developed which can successfully treat the three-body Coulomb continuum problem and thus make accurate predictions for direct ionization cross sections. For electron scattering from a hydrogen atom, the converged close coupling [1], the hyperspherical close-coupling [2], the *R*-matrix pseudostates [3], the time-dependent close coupling [4], and the exterior complex scaling [5] methods have all produced total integrated ionization cross sections in excellent agreement with experimental measurements [6].

Recently the time-dependent close-coupling method has been used to calculate the direct electron-impact ionization cross section for the quasi-one-electron targets found in the lithium [7,8] and sodium [9] isoelectronic sequences. Although the time-dependent close-coupling results are in reasonably good agreement with the converged close-coupling and *R*-matrix pseudostates results, the overall agreement between nonperturbative theory and some of the older experiments is less than satisfactory. New experiments on B^{2+} [10] and Al^{2+} [11] are now in much better agreement with the predictions of the nonperturbative methods.

In this paper we extend the formulation of the time-dependent close-coupling method to calculate the direct electron-impact ionization cross section of helium. This is an important first step in the eventual application of this particular nonperturbative method to the direct ionization of all open and closed shell atomic systems. In a frozen core approximation, the wave function for the three-electron system is expanded in terms of two-electron wave functions which fully describe the ejected and scattered electrons at all times following the collision. Reduction of the time-dependent Schrödinger equation yields coupled sets of partial differential equations for two-electron radial wave functions which include a direct and a local approximation to the exchange interactions with the remaining core electron. Through unitarity considerations, total integrated cross sections may be obtained by direct projection of the time-dependent wave functions onto either bound or continuum lattice eigenstates. In contrast to previous work on the $L=0$ model for hydrogen [12,13], we now find that ejected energy differential cross sections are most effectively calculated by direct projection onto the continuum lattice eigenstates. The new extension of the time-dependent close-coupling method is presented in Sec. II, the integrated and differential ionization cross sections for helium are presented in Sec. III, and a brief summary is found in Sec. IV.

II. THEORY

For electron scattering from a helium atom, the nonrelativistic Hamiltonian (in atomic units) is given by

$$H=\sum_{i=1}^{3}\left(-\frac{1}{2}\nabla_i^2-\frac{Z}{r_i}\right)+\sum_{i<j=1}^{3}\frac{1}{|\vec{r}_i-\vec{r}_j|}, \tag{1}$$

where $\vec{r}_i$ are the coordinates of the electrons and $Z=2$ is the atomic number. The total wave function for a given $\mathcal{LS}$ symmetry may be expanded in coupled spherical harmonics:

$$\Psi^{\mathcal{LS}}(\vec{x}_1,\vec{x}_2,\vec{x}_3,t)=\mathcal{A}_{12}\mathcal{A}_{13}\mathcal{A}_{23}\sum_{L,S}\sum_{l_1,l_2,l_3}\frac{P^{\mathcal{LS}}_{l_1l_2l_3LS}(r_1,r_2,r_3,t)}{r_1r_2r_3}\times W((l_1,(l_2,l_3)L)\mathcal{L}M_{\mathcal{L}})W((s_1,(s_2,s_3)S)\mathcal{S}M_{\mathcal{S}}), \tag{2}$$

where the three electron coupling operators *W* are themselves coupled products involving two electron coupling operators given by

$$W((l,l')LM_L)=\sum_{m_l,m_{l'}}C^{ll'L}_{m_lm_{l'}M_L}Y_{lm_l}(\Omega)Y_{l'm_{l'}}(\Omega'), \tag{3}$$

and

$$W((s,s')SM_S)=\sum_{m_s,m_{s'}} C^{ss'S}_{m_s m_{s'} M_S}\chi_{m_s}(\sigma)\chi_{m_{s'}}(\sigma'). \quad (4)$$

In Eqs. (2)–(4), $\mathcal{A}_{ij}$ is an antisymmetrization operator, $C^{l_1 l_2 l_3}_{m_1 m_2 m_3}$ is a Clebsch-Gordan coefficient, $Y_{lm}(\Omega)$ is a spherical harmonic, and $\chi_m(\sigma)$ is a spinor. Reduction of the time-dependent Schrödinger equation yields a set of time-dependent close-coupled partial differential equations for each $\mathcal{LS}$ symmetry involving the three dimensional radial wave functions, $P^{\mathcal{LS}}_{l_1 l_2 l_3 LS}(r_1,r_2,r_3,t)$, of Eq. (2). The full three-dimensional radial solutions are needed for electron double ionization of helium near threshold [14], so that the correlated quantal dynamics of three free electrons moving in the long-range Coulomb field of a fourth body may be accurately described.

For electron single ionization of helium near threshold, the total wave function for a given $\mathcal{LS}$ symmetry may be expanded in coupled spherical harmonics using a frozen core approximation:

$$\Psi^{\mathcal{LS}}(\vec{x}_1,\vec{x}_2,\vec{x}_3,t)=\mathcal{A}_{12}\mathcal{A}_{13}\sum_{L,S}\frac{P_{n_1 l_1}(r_1)}{r_1}\psi^{LS}(\vec{x}_2,\vec{x}_3,t) \times W((l_1,L)\mathcal{L}M_{\mathcal{L}})W((s_1,S)\mathcal{S}M_{\mathcal{S}}), \quad (5)$$

where the two-electron wavefunctions are given by

$$\psi^{LS}(\vec{x}_2,\vec{x}_3,t)=A_{23}\sum_{l_2,l_3}\frac{P^{LS}_{l_2 l_3}(r_2,r_3,t)}{r_2 r_3} \times W((l_2,l_3)LM_L)W((s_2,s_3)SM_S). \quad (6)$$

The two-dimensional radial solutions are needed so that the correlated quantal dynamics of two free electrons moving in the long-range Coulomb field of a third body may be accurately described. If we restrict ourselves to electron scattering from the ground state of helium (i.e., $n_1 l_1 = 1s$) and assume no exchange scattering with the core electron (i.e., $\mathcal{A}_{12}=\mathcal{A}_{13}=1$), then reduction of the time-dependent Schrödinger equation yields the following set of time-dependent close-coupled partial differential equations for each LS symmetry:

$$i\frac{\partial P^{LS}_{l_2 l_3}(r_2,r_3,t)}{\partial t}=T_{l_2 l_3}(r_2,r_3)P^{LS}_{l_2 l_3}(r_2,r_3,t) + \sum_{l_2',l_3'} U^{L}_{l_2 l_3, l_2' l_3'}(r_2,r_3)P^{LS}_{l_2' l_3'}(r_2,r_3,t), \quad (7)$$

where

$$T_{l_2 l_3}(r_2,r_3)=-\frac{1}{2}\frac{\partial^2}{\partial r_2^2}-\frac{1}{2}\frac{\partial^2}{\partial r_3^2}+\frac{l_2(l_2+1)}{2r_2^2}+\frac{l_3(l_3+1)}{2r_3^2} -\frac{Z}{r_2}+V_D(r_2)-\frac{Z}{r_3}+V_D(r_3), \quad (8)$$

and the coupling operator is given by

$$U^{L}_{l_2 l_3, l_2' l_3'}(r_2,r_3) =(-1)^{L+l_3+l_3'}\sqrt{(2l_2+1)(2l_2'+1)(2l_3+1)(2l_3'+1)} \times\sum_{\lambda}\frac{r_<^{\lambda}}{r_>^{\lambda+1}}\begin{pmatrix} l_2 & \lambda & l_2' \\ 0 & 0 & 0\end{pmatrix}\begin{pmatrix} l_3 & \lambda & l_3' \\ 0 & 0 & 0\end{pmatrix}\begin{Bmatrix} L & l_3' & l_2' \\ \lambda & l_2 & l_3\end{Bmatrix}. \quad (9)$$

In Eq. (6) the ''direct'' potential terms are given by

$$V_D(r)=\int_0^{\infty}\frac{P^2_{1s}(r_1)}{\max(r_1,r)}dr_1 \quad (10)$$

and act to shield the outer active electrons (with coordinates $\vec{r}_2$ and $\vec{r}_3$) from the full Coulomb attraction of the nucleus.

If the antisymmetrization operators $\mathcal{A}_{12}$ and $\mathcal{A}_{13}$ are included in the total wave function of Eq. (5), the resulting time-dependent close-coupling equations for s-wave core scattering will include further ''exchange'' potential terms in $T_{l_2 l_3}(r_2,r_3)$ of Eq. (8). We approximate those nonlocal terms using a semiempirical potential given by [15]

$$V_X(r)=-\alpha\left(\frac{24\rho_{1s}(r)}{\pi}\right)^{1/3}, \quad (11)$$

where α is a parameter determined by removal energies and $\rho_{1s}(r)=P^2_{1s}/4\pi r^2$ is the radial probability density.

The frozen-core radial orbital of Eq. (5) is calculated as the hydrogenic ground state radial orbital of He^+. This orbital provides a precise description for the final state of the ionized target with two escaping electrons. A set of single particle radial orbitals $\overline{P}_{nl}(r)$, are obtained by diagonalization of the single particle Hamiltonian given by

$$h(r)=-\frac{1}{2}\frac{\partial^2}{\partial r^2}+\frac{l(l+1)}{2r^2}-\frac{Z}{r}+V_D(r)+V_X(r). \quad (12)$$

The parameter α in the exchange term is adjusted so that the single particle energies for each angular momentum are in reasonable agreement with the configuration-average experimental spectrum. The $\overline{P}_{1s}(r)$ radial orbital with energy $\epsilon_{1s}=-24.6$ eV is very similar to the Hartree-Fock ground state radial orbital of He.

The two-electron radial wave functions of Eq. (6) at time $t=0$ are constructed according to

$$P^{LS}_{l_2 l_3}(r_2,r_3,t=0)=\sqrt{\frac{1}{2}}[G_{k_2 l_2}(r_2)\delta_{0,l_3}\overline{P}_{1s}(r_3) + (-1)^S\delta_{0,l_2}\overline{P}_{1s}(r_2)G_{k_3 l_3}(r_3)], \tag{13}$$

where k is the linear momentum and $G_{kl}(r)$ is a radial wave packet. The factor $(-1)^S$ assures overall antisymmetry for the two-electron wave function. We employ a simple ''staggered leapfrog'' approximation [16] to time propagate the time-dependent close-coupling equations for each LS symmetry.

The two-electron radial wave functions at a time $t=T$ following the collision are projected onto products of single particle continuum radial orbitals to yield the momentum space probabilities given by

$$\mathcal{P}^{LS}_{k_2 l_2 k_3 l_3} = \left| \int_0^\infty dr_2 \int_0^\infty dr_3 \overline{P}_{k_2 l_2}(r_2)\overline{P}_{k_3 l_3}(r_3)P^{LS}_{l_2 l_3}(r_2,r_3,t=T)\right|^2. \tag{14}$$

In the (k_2,k_3) plane the momentum space probabilities are peaked along the line of total energy $\mathcal{E}=k_2^2/2+k_3^2/2=k_0^2/2-I_p$, where I_p is the ionization potential of the atom. The diagonalization of $h(r)$ of Eq. (12) on the lattice determines the density of states. The (k_2,k_3) plane may be divided into angular segments specified by the hyperspherical angle, $\tan(\theta)=k_3/k_2$. The differential cross section in hyperspherical angle is given by

$$\frac{\Delta\sigma}{\Delta\theta}=\frac{\pi}{2k_0^2\Delta\theta}\sum_{L,S}(2L+1)(2S+1)\sum_{k_2,k_3}{}'\sum_{l_2,l_3}\mathcal{P}^{LS}_{k_2 l_2 k_3 l_3}, \tag{15}$$

where the sum over linear momentums is restricted to be within a certain angular sector $\Delta\theta$ given by

$$\theta-\frac{\Delta\theta}{2}<\tan^{-1}\left(\frac{k_3}{k_2}\right)<\theta+\frac{\Delta\theta}{2}. \tag{16}$$

The differential cross section in ejected energy ($\epsilon=k_2^2/2$) is given by

$$\frac{d\sigma}{d\epsilon}=\frac{1}{k_2 k_3}\frac{d\sigma}{d\theta}, \tag{17}$$

and the total cross section is given by

$$\sigma=\int_0^{\mathcal{E}}\frac{d\sigma}{d\epsilon}d\epsilon. \tag{18}$$

Through unitarity considerations, a bound-state projection operator may also be used to extract ionization probabilities from the two-electron radial wave functions at a time $t=T$ following the collision. The method is more efficient for extracting total integrated cross sections, but is very slowly convergent in lattice box size for extracting ejected energy differential cross sections [13]. In the latter case, we strongly recommend the continuum state projection method outlined above.

TABLE I. Partial ionization cross sections (10^{-18} cm^2) for helium from the time-dependent close-coupling method (E is the incident energy and L is the total angular momentum).

L	$E=75$ eV	$E=100$ eV	$E=150$ eV	$E=200$ eV
0	2.26	1.86	1.27	0.92
1	3.75	3.23	2.34	1.76
2	6.73	5.55	3.76	2.72
3	6.65	6.18	4.63	3.47
4	5.23	5.56	4.72	3.74
5	3.57	4.36	4.25	3.60
6	2.32	3.21	3.58	3.26

III. CROSS-SECTION RESULTS

For electron scattering from a helium atom, the time-dependent close-coupled partial differential equations [see Eq. (7)] are solved on a 250×250 point lattice with each radial direction from 0 to 50 a.u. spanned by a uniform mesh with spacing $\Delta r=0.2$ a.u. The initial radial wave packet, $G_{kl}(r)$ of Eq. (13), is centered at 25 a.u. from the nucleus with a full width at half maximum of 6.25 a.u. Propagation times depend solely on the initial incident energy, $E=k_0^2/2$, from a total time of $T=23$ a.u. for $E=75$ eV to $T=15$ a.u. for $E=200$ eV. The actual number of numerical time steps depends on the initial incident energy and the LS symmetry, from 11 500 time steps for $^{1,3}I$ symmetry at $E=75$ eV to 3000 time steps for $^{1,3}S$ symmetry at $E=200$ eV. The number of coupled channels ($l_2 l_3$ values) ranged from 4 for $^{1,3}S$ symmetry to 16 for $^{1,3}I$ symmetry. For example, the 12 coupled channels for $^{1,3}F$ symmetry have $l_2 l_3$ values of (0,3), (3,0), (1,2), (2,1), (1,4), (4,1), (2,3), (3,2), (2,5), (5,2), (3,4), and (4,3), in accordance with rules governing the addition of angular momenta. The full lattice was partitioned over 25 distributed memory computing processors, so that each processor time evolved in parallel the coupled radial wave functions on a 250×10 point sublattice. The only communication needed is that of the kinetic energy on the boundaries.

Partial ionization cross sections for electron scattering from helium calculated in the time-dependent close-coupling method are presented in Table I. We also carried out time-independent distorted-wave calculations based on a triple partial-wave expansion of the first-order perturbation theory scattering amplitude, including both direct and exchange terms. The incident and scattered electrons are calculated in a V^N potential, while the bound and ejected electrons are calculated in a V^{N-1} potential [17]. The bound electron is represented by a Hartree-Fock ground-state radial orbital of He, and the phase between the direct and exchange terms in the scattering amplitude is determined by the angular algebra (the so-called ''natural'' phase). Partial ionization cross sec-

TABLE II. Partial ionization cross sections (10^{-18} cm^2) for helium from the distorted-wave with exchange method (E is the incident energy and L is the total angular momentum).

L	$E=75$ eV	$E=100$ eV	$E=150$ eV	$E=200$ eV
0	2.52	1.96	1.16	0.75
1	2.72	2.39	1.68	1.21
2	9.24	6.85	3.96	2.57
3	8.14	7.34	5.03	3.48
4	6.05	6.38	5.12	3.83
5	4.13	4.99	4.64	3.75
6	2.66	3.68	3.90	3.40
7-30	4.37	8.54	13.84	15.76
0-30	39.82	42.12	39.34	34.73

tions for electron scattering from helium for this particular distorted-wave method are presented in Table II. The overall agreement between the perturbative and nonperturbative calculations for the partial ionization cross sections for electron scattering from helium is reasonably good. For other atoms, and for other formulations of the first-order distorted-wave method, we do not expect to find such good agreement, especially for low total angular momentum.

Total ionization cross sections for electron scattering from helium are presented in Fig. 1. The solid and dashed curves are perturbative distorted-wave results with and without exchange terms in the scattering amplitude. The solid squares are hybrid results: nonperturbative close coupling for $L=0-6$ and perturbative distorted wave for $L=7-30$. We find excellent agreement between the hybrid results and the experimental measurements of Montague *et al.* [18] The time-dependent close-coupling cross sections, topped up at high angular momentum with distorted-wave results, are also in excellent agreement with previous converged close-coupling [19] and R-matrix pseudostates [20] calculations for the total

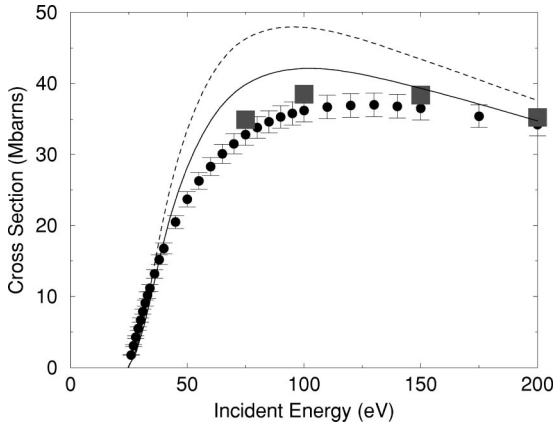

FIG. 1. Total electron-impact ionization cross section for helium. Solid squares: time-dependent close-coupling method, topped up at high angular momentum with distorted-wave results, solid curve: distorted-wave with exchange method, dashed curve: distorted-wave with no exchange method, solid circles: experimental measurements [18] ($1.0\,\mathrm{Mb}=1.0\times10^{-18}\,\mathrm{cm}^2$).

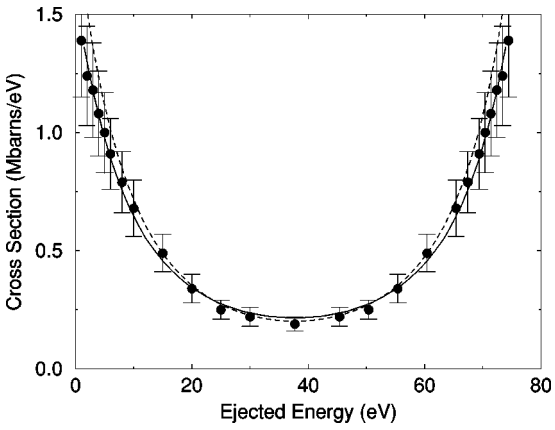

FIG. 2. Ejected-energy differential electron-impact ionization cross section for helium at an incident energy of 100 eV. Solid curve: time-dependent close-coupling method, topped up at high angular momentum with distorted-wave results, dashed curve: distorted-wave with exchange method, solid circles: experimental measurements [23] ($1.0\,\mathrm{Mb}=1.0\times10^{-18}\,\mathrm{cm}^2$).

ionization cross section of helium. Subsequent experiments [21,22] have confirmed the original measurements reported by Montague *et al.* [18].

Ejected-energy differential ionization cross sections, at an incident energy of 100 eV, for electron scattering from helium are presented in Fig. 2. The time-dependent close-coupling results, topped up at high angular momentum with distorted-wave results, are given by the solid curve, while the distorted-wave with exchange results are given by the dashed curve. Both theoretical predictions are in excellent agreement with the ''derived'' experimental measurements of Shyn and Sharp [23]. The ''raw'' experimental measurements are for the double differential cross section. We integrated the ''raw'' measurements over the scattering angle to obtain single differential cross sections in ejected energy and then redefined the cross section for a range of 0 to $\mathcal{E}$ by dividing by 2. A further integration over ejected energy yielded a total ionization cross section at 100 eV that was 25% larger than the experimental normalization value of $3.54\times10^{-17}\,\mathrm{cm}^2$ [23]. We then renormalized the single differential cross sections so that their integrated value is indeed $3.54\times10^{-17}\,\mathrm{cm}^2$. The resulting ''derived'' measurements are the ones compared to theory in Fig. 2. Once the experimental normalization is corrected, the time-dependent close-coupling results, previous converged close-coupling results [24], and the Shyn and Sharp experimental measurements are all found to be in excellent agreement.

IV. SUMMARY

Direct ionization cross sections for electron scattering from a helium atom are calculated using an extension of a time-dependent close-coupling method developed for one-electron targets [4,7]. The resulting close-coupled partial differential equations for the two-electron radial wave functions

describing the ejected and scattered electrons contain a direct and a local approximation to the exchange interactions with the remaining core electron. Total integrated and ejected energy differential ionization cross sections are found to be in excellent agreement with experimental measurements. Future plans include calculations of other positive and negative ions in the helium isoelectronic sequence, as well as further extensions of the theory for the treatment of other open and closed shell atomic systems.

ACKNOWLEDGMENTS

We would like to thank Dr. Mark Baertschy, Dr. Dario Mitnik, Dr. Bill McCurdy, and Dr. Don Griffin for several useful discussions. This work was supported in part by the U.S. Department of Energy and the National Science Foundation. Computational work was carried out at the National Energy Research Supercomputer Center in Berkeley, California.

[1] I. Bray and A. T. Stelbovics, Phys. Rev. Lett. **70**, 746 (1993).
[2] D. Kato and S. Watanabe, Phys. Rev. Lett. **74**, 2443 (1995).
[3] K. Bartschat and I. Bray, J. Phys. B **29**, L577 (1996).
[4] M. S. Pindzola and F. Robicheaux, Phys. Rev. A **54**, 2142 (1996).
[5] M. Baertschy, T. N. Rescigno, C. W. McCurdy, and W. A. Isaacs, Bull. Am. Phys. Soc. **44**, 501 (1999).
[6] M. B. Shah, D. S. Elliot, and H. B. Gilbody, J. Phys. B **20**, 3501 (1987).
[7] M. S. Pindzola, F. Robicheaux, N. R. Badnell, and T. W. Gorczyca, Phys. Rev. A **56**, 1994 (1997).
[8] D. M. Mitnik, M. S. Pindzola, D. C. Griffin, and N. R. Badnell, J. Phys. B **32**, L479 (1999).
[9] N. R. Badnell, M. S. Pindzola, I. Bray, and D. C. Griffin, J. Phys. B **31**, 911 (1998).
[10] O. Woitke, N. Djuric, G. H. Dunn, M. E. Bannister, A. C. H. Smith, B. Wallbank, N. R. Badnell, and M. S. Pindzola, Phys. Rev. A **58**, 4512 (1998).
[11] J. W. G. Thomason and B. Peart, J. Phys. B **31**, L201 (1998).
[12] F. Robicheaux, M. S. Pindzola, and D. R. Plante, Phys. Rev. A **55**, 3573 (1997).
[13] M. S. Pindzola and F. Robicheaux, Phys. Rev. A **55**, 4617 (1997).
[14] M. S. Pindzola, D. Mitnik, and F. Robicheaux, Phys. Rev. A **59**, 4390 (1999).
[15] R. D. Cowan, *The Theory of Atomic Structure and Spectra* (University of California Press, Berkley, 1981), p. 199.
[16] W. H. Press, S. A. Teukolsky, W. T. Vetterling, and B. P. Flannery, *Numerical Recipes* (Cambridge University Press, Cambridge, 1992), p. 833.
[17] S. M. Younger, Phys. Rev. A **22**, 111 (1980).
[18] R. K. Montague, M. F. A. Harrison, and A. C. H. Smith, J. Phys. B **17**, 3295 (1984).
[19] D. V. Fursa and I. Bray, Phys. Rev. A **52**, 1279 (1995).
[20] E. T. Hudson, K. Bartschat, M. P. Scott, P. G. Burke, and V. M. Burke, J. Phys. B **29**, 5513 (1996).
[21] R. C. Wetzel, F. A. Baiocchi, T. R. Hayes, and R. S. Freund, Phys. Rev. A **35**, 559 (1987).
[22] M. B. Shah, D. S. Elliott, P. McCallion, and H. B. Gilbody, J. Phys. B **21**, 2751 (1988).
[23] T. W. Shyn and W. E. Sharp, Phys. Rev. A **19**, 557 (1979).
[24] I. Bray and D. V. Fursa, J. Phys. B **28**, L435 (1995).